

# Saturated area formation on nonconvergent hillslope topography with shallow soils: A numerical investigation

Fred L. Ogden and Brent A. Watts<sup>1</sup>

Department of Civil and Environmental Engineering, University of Connecticut, Storrs

**Abstract.** Prediction of saturated area formation is important for hydrologic modeling of watersheds with shallow, highly pervious soils. This simulation study examines the relative importance of hillslope properties and rainfall rate on the evolution of saturated source areas during wetting. The study focuses on homogeneous, nonconvergent hillslope topography with constant slope. The two-dimensional, variably saturated groundwater model VS2D [Healy, 1990; Lappala *et al.* 1993] is used to simulate saturated area formation under the action of steady uniform rainfall. The study methodology systematically varies four hillslope properties, depth to impervious layer, slope length, slope angle, and average saturated hydraulic conductivity, and the rainfall rate. Results indicate that the fraction of the hillslope length that is saturated at equilibrium is a function of a parameter  $\Phi$ , which is defined as the rainfall rate multiplied by the slope length, divided by the slope angle, soil thickness, and saturated hydraulic conductivity. The temporal evolution of saturated area is analyzed in terms of the equilibrium time. Nonlinearity in the unsaturated zone and differences in hillslope properties result in a nonunique time to equilibrium relation. The time to equilibrium is maximum when factors that tend to cause surface saturation are in approximate balance with those that tend to dissipate surface saturation. The temporal evolution of surface saturation during wetting follows a wide variety of trajectories. Equivalent hillslope soil water storage ratios on slopes with different properties can result in a wide range of surface saturation conditions. Hillslopes with shallower soils and smaller slope angles are most susceptible to saturated area formation. However, sudden changes in surface saturation are possible on steep hillslopes when  $1 < \Phi < 6$ .

## 1. Introduction

It is improper to apply Hortonian models to watersheds in humid regions with shallow, highly pervious soils because of the significant role that groundwater plays in runoff production. In contrast to the infiltration excess “Hortonian” [Horton, 1933] model, runoff in humid regions with coarse-textured soils is generated by saturation from below by a rising groundwater table. Subsurface flow saturates the soil near the toe of a slope, and overland flow occurs when rain falls on the saturated areas. Saturation at the toe of the slope often develops because of a break in the slope that reduces the hydraulic potential gradient or because the slope intersects a free water surface such as a stream. This is commonly referred to as the saturation excess runoff production mechanism. The saturated areas at the bottom of the slope are called variable source areas or saturated source areas (SSAs). Runoff generated from these areas is called saturation excess runoff. Runoff modeling in humid regions is complicated by the influence of subsurface conditions on runoff production. Many models of saturation excess runoff have conceptual formulations that lump subsurface parameters in space [Watts, 1998]. Models of this type do not allow detailed study of the influence of fine-scale spatial variability in land-surface characteristics and rainfall on runoff production.

<sup>1</sup>Now at Nantucket, Massachusetts.

Copyright 2000 by the American Geophysical Union.

Paper number 2000WR900091.  
0043-1397/00/2000WR900091\$09.00

## 2. Literature Review

In many vegetated areas of the northeastern United States the infiltration capacity of the soils is not exceeded in all but the most extreme rainfall events. Infiltration capacities are high for a number of reasons. Vegetation protects the soil from rain packing and dispersal [Kirkby, 1978]. Glacial soils that are predominant in the northeastern United States have low clay and a high sand/gravel content. Furthermore, the combined effects of dense forest litter, shallow root mats, and faunal activity greatly increase the permeability of the upper soil horizon.

Researchers in the 1960s, using data collected in experimental watersheds [Southeastern Forest Experiment Station, 1961; Tennessee Valley Authority, 1965; Hewlett and Hibbert, 1967], theorized a new type of runoff production mechanism that is more applicable to humid areas than the Hortonian concept. Termed “saturation excess overland flow” this runoff production mechanism depends on surface saturation of a small portion of the watershed. Saturated areas expand during rainfall and can behave hydrologically as impervious surfaces under the action of rainfall.

One of the first researchers to identify the partial area mechanism was Betson [1964]. Betson used a nonlinear mathematical model, which incorporated Horton’s [1933] runoff generation mechanism, to analyze the runoff from a number of basins in Tennessee. Betson concluded that the percentage of area contributing to runoff on 14 basins of different sizes ranged from 5% to 36%. Betson concluded that in certain geographic areas, storm runoff frequently occurs from only a small portion of the watershed.

*Dunne and Black* [1970] extended Betson's ideas using data collected at the Sleepers River experimental watershed in Vermont. This experimental watershed is located in an area with highly permeable soils and frequent, low-intensity rainfall. Data analyzed by *Dunne and Black* [1970] included measurements of rainfall, runoff, water table elevations, and soil moisture. *Dunne and Black* [1970] concluded that the runoff production mechanism described by *Horton* [1933] did not occur at Sleepers River and that overland flow was generated on small areas of the watershed where the water table had risen to the ground surface. It is this type of overland flow that contributes significant amounts of direct runoff to streamflow during storm events in watersheds with highly permeable soils. Variable source areas are generally found in valley bottoms, along streams, in convergent topography, and in swales. Subsurface conditions can also cause saturated zones to occur in upland regions of the basin [*Bras*, 1990]. A comprehensive summary of the saturation excess runoff concept is given by *Chorley* [1978], *O'Brien* [1983], and *Anderson and Burt* [1990].

Considerable research has been conducted to predict the formation of SSAs. Several researchers have extended the concepts developed by *Dunne and Black* [1970]. *Freeze* [1972] used a deterministic mathematical model that coupled channel flow and variably saturated subsurface flow to investigate saturation excess contributions. *Freeze* [1972] concluded that on concave slopes with lower permeabilities, and on all convex slopes, surface saturation occurred because of rising water tables rather than from lateral subsurface flow.

*Beven and Kirkby* [1979] developed the saturation excess model TOPMODEL from topographic-based considerations. TOPMODEL uses distributed input; however, it is essentially a lumped parameter model along lines of constant parameter  $\ln(a)/\tan(B)$ , where  $a$  is the area drained per unit contour length at a point and  $\tan(B)$  is the local land-surface slope. TOPMODEL has been further developed and applied to numerous engineering and research projects [*Hornberger et al.*, 1985; *Wolock et al.*, 1989; *Iorgulescu and Jordan*, 1994; *Obled et al.*, 1994; *McDonnell et al.*, 1996].

*O'Loughlin* [1981] developed analytical relationships to predict the amount of surface saturation using two hillslope models. *O'Loughlin* [1981] used one model with a horizontal impermeable layer and another with a sloping impermeable layer. Assuming a hydrostatic pressure distribution, *O'Loughlin* [1981] integrated over the saturated area and solved for the groundwater intercept. The groundwater intercept determined the location of the saturated area. *O'Loughlin* [1981] concluded that for slopes with horizontal impermeable layers, the size of the saturated slope was proportional to  $q S_o^{-2} K_s^{-1}$ , where  $q$  is the base flow,  $S_o$  is the slope angle, and  $K_s$  is the saturated hydraulic conductivity. The amount of slope saturated for hillslopes with a sloping impermeable layer was proportional to  $\{((q S_{o1}^{-1} S_{o2}^{-1} K_s^{-1} \ln[f(q, S_{o1}, S_{o2}, K_s)])\}$ , where  $S_{o1}$  is the slope of the impermeable layer and  $S_{o2}$  is the slope of the land surface. *O'Loughlin* [1981] also investigated the influence of converging and diverging hillslopes on the development of saturated areas. Using a topographic model that was a function of hillslope height, *O'Loughlin* [1981] determined that converging flow zones produced seepage boundaries that are more stable under varying drainage conditions than their counterparts for parallel and diverging flow zones.

*O'Loughlin* [1986] developed the program WETZONE to determine saturated areas within two catchments. WETZONE solves a wetness function everywhere in the catchment. Results

showed that the amount of rapid surface runoff was dependent on the value of a normalized wetness parameter. A number of researchers have applied numerical models to study saturation excess runoff at the hillslope scale. *Neiber and Walter* [1981] applied a two-dimensional finite element unsaturated flow model to duplicate laboratory-scale observations. *Beven* [1981] developed a kinematic-wave model of saturated flow in hillslopes. Neither of these researchers focused on the temporal evolution of saturated source areas during wetting.

Two more recently developed procedures for determining saturation excess runoff are from *Boughton* [1990] and *Steenhuis et al.* [1995]. *Boughton's* [1990] procedure is intensive in that the method is based on the identification of portions of the watershed that contribute to surface runoff by analyzing rainfall and runoff records. *Boughton's* [1990] analysis of a 15-year period of record showed that two thirds of direct runoff originated from 15% of the watershed area that has the smallest surface storage capacity. In an effort to find a simple engineering method to predict direct runoff from saturated areas, *Steenhuis et al.* [1995] showed that the U.S. Department of Agriculture Natural Resources Conservation Service (formerly Soil Conservation Service (SCS)) runoff equation can be interpreted in a form suitable for simulating saturation excess runoff production. *Steenhuis et al.* [1995] performed a basic analysis of the procedure and found that the SCS curve number equation in its elementary form performs adequately when appropriate parameter values are applied. Models of saturation excess runoff that are currently widely used are largely of the conceptual, lumped-parameter type [*Watts*, 1998]. Models of this type do not incorporate hydrologic parameters in a truly distributed sense as do physically based models; rather, topographic position in the landscape is used as an indicator of other parameters.

Recent physics-based models of saturation excess runoff include the model by *Wigmosta et al.* [1994], which is noted for its completeness, the Soil Moisture-Based Runoff Model SmoR-Mod [*Zollweg et al.*, 1996], and the model by *Frankenberger et al.* [1999]. These models are significant in that they have physically based formulations and represent the spatial variability of watershed characteristics. General results are difficult to obtain from field and laboratory studies of hillslope processes. Results obtained in field studies are ultimately site-dependent, and laboratory studies are very time-consuming. Both *Nieber and Walter* [1981] and *Barros et al.* [1999] performed laboratory studies of runoff production in shallow soils at small-plot scales in the laboratory.

Placing soil in laboratory test plots to promote homogeneity and eliminate preferential flow paths, developing consistent initial conditions, and accurately simulating rainfall fluxes are all problematic in the laboratory. Furthermore, accurately measuring the moisture content of the upper soil layer to determine saturated source area is very difficult. A numerical approach using a robust two-dimensional model of unsaturated flow is justified. Performing this study in a laboratory would be prohibitively time-consuming and expensive.

### 3. Objectives

Detailed understanding of the importance of hillslope properties and rainfall on the temporal evolution of saturated source area will aid in further development of physically based saturation excess runoff models. The objective of this research is to explore the relationship between physically based hillslope properties and rainfall rate on the temporal evolution of sat-

urated surface area on a uniform, hypothetical hillslope. This objective is accomplished using a two-dimensional variable-saturation subsurface model to simulate the response of a topographically nonconvergent, constant-slope hillslope. The response time of SSA production is considered relative to the time to equilibrium  $t_e$  for each set of hillslope characteristics examined. Model sensitivity to each input is analyzed, allowing identification of the role of hillslope and rainfall properties on SSA formation. Fundamental analytical relations are derived and applied to analyze simulation results.

#### 4. Governing Equations and Modeling Technique

The movement of liquid water in variably saturated porous media is described by combining the conservation of mass for water with Darcy's law and an auxiliary storage equation. Given an elementally control volume (CV) of soil, bounded by control surfaces (CS), the conservation of mass for liquid water requires that the following equation be satisfied:

$$\frac{\partial}{\partial t} \iiint \rho_w \theta \, dV + \iint \rho_w \hat{u}_n \, dA - \iiint \rho_w q \, dV = 0, \quad (1)$$

where

- $\rho_w$  liquid density of water ( $M L^{-3}$ );
- $\theta$  volumetric water content ( $L^0$ );
- $t$  time ( $T$ );
- $\hat{u}_n$  liquid flux per unit area in the direction  $n$ , which is normal to  $dA$  ( $L T^{-1}$ );
- $q$  source-sink term accounting for water added ( $+q$ ) or taken away ( $-q$ ) from the control volume ( $T^{-1}$ ).

Assuming that  $dV$  is small enough that density ( $\rho_w$ ) and volumetric water content ( $\theta$ ) can be considered "representative" values, (1) can be simplified as

$$V \frac{\partial(\rho_w \theta)}{\partial t} + \iint \rho_w \hat{u}_n \, dA - \rho_w q V = 0. \quad (2)$$

Assuming that the fluid flux normal to the surface  $A$  bounding  $V$  is described by Darcy's law extended to variably saturated conditions, the following equation results:

$$\hat{u}_n = -K(h) \frac{\partial H}{\partial n}, \quad (3)$$

where  $K(h)$  is unsaturated hydraulic conductivity as a function of pressure head ( $L T^{-1}$ ),  $h$  is pressure head ( $L$ ), and  $H$  is total head, under variably saturated conditions,  $H = h + h_z$ , where  $h_z$  is elevation head ( $L$ ).

The *van Genuchten* [1980] equation was used to predict the soil hydraulic conductivity and capillary head based on soil water content. This relation was selected for use in this study because it has a continuous slope and works well at higher degrees of saturation [Bras, 1990].

Substituting (3) into (2) gives the following result:

$$V \frac{\partial(\rho_w \theta)}{\partial t} + \iint \rho_w K(h) \frac{\partial H}{\partial n_k} \, dA - \rho_w q V = 0. \quad (4)$$

If all the quantities under the surface integral can be considered constant over each of  $m$  faces of the general polygonal volume  $V$ , (4) can be approximated by

$$V \frac{\partial(\rho_w \theta)}{\partial t} + \sum_{k=1}^m \rho_w K(h) A_k \frac{\partial H}{\partial n_k} - \rho_w q V = 0, \quad (5)$$

where  $A_k$  is the area of the  $k$ th face to which  $n_k$  is normal.

Liquid water held in storage is expressed by the first term in (5) and can be expanded as follows using the product rule:

$$V \frac{\partial(\rho_w s \phi)}{\partial t} = V \left[ \rho_w \phi \left( \frac{\partial s}{\partial t} \right) + \rho_w s \left( \frac{\partial \phi}{\partial t} \right) + s \phi \left( \frac{\partial \rho_w}{\partial t} \right) \right], \quad (6)$$

where  $\phi$  is porosity ( $L^0$ ) and  $s$  is relative saturation equal to  $\theta/\phi$  ( $L^0$ ). The three terms in parentheses on the right-hand side of (6) account for changes in liquid stored in  $V$  owing to (1) changes in liquid saturation, (2) compression or expansion of pore space of the porous medium, and (3) compression or expansion of the liquid. Compression of the fluid and media are not important for this problem but are included in (6) for completeness.

Because the principal dependent variable used in the model is total head  $H$ , the relevant storage term is written in terms of  $H$ , assuming constant  $\phi$  and  $\rho_w$  to yield

$$V \frac{\partial \theta}{\partial t} = V \frac{\partial \theta}{\partial H} \frac{\partial H}{\partial t}. \quad (7)$$

The water content  $\theta$  is taken to be independent of all components of  $H$  except the pressure potential  $h$ . Substituting (7) into (5) yields the nonlinear flow equation for variably saturated porous media, which is written for each volume element within the solution domain:

$$V c_m \frac{\partial H}{\partial t} + \sum_{k=1}^m K(h) A_k \frac{\partial H}{\partial n_k} - q V = 0, \quad (8)$$

where  $c_m = \partial \theta / \partial h$  equals specific moisture capacity, the slope of the moisture retention curve ( $L^{-1}$ ).

The model VS2D, developed at the United States Geological Survey by *Healy* [1990] and *Lappala et al.* [1993], is used in this study to solve (8). VS2D is a two-dimensional unsteady model of saturated/unsaturated flow. VS2D uses the strongly implicit procedure [Stone, 1968] finite difference solution technique and was developed to simulate "difficult" nonlinear problems, such as those caused by infiltration into dry soils and by discontinuities in permeability and porosity. VS2D is capable of performing model simulations in either rectangular or cylindrical coordinates. At the outset of this study it was thought that cylindrical coordinates would allow simulations of converging and diverging hillslope topography. The cylindrical coordinate feature in VS2D is not applicable because it does not allow a slope angle when using cylindrical coordinates. Three different soil moisture retention relationships can be used in VS2D, *Brooks and Corey* [1964], *Haverkamp et al.* [1977], and *van Genuchten* [1980] or laboratory data.

VS2D allows several different boundary conditions including constant flux, constant head, and seepage faces. Seepage faces are areas along the model boundary where if the head is greater than the boundary height, exfiltration occurs. VS2D also has options to model solute transport, evapotranspiration, and evaporation; these features were not used in this study. Complete details of the model, including validation study results, are published in the VS2D user's manual [Lappala et al., 1993]. VS2D was applied by *Halford* [1997] and found to match time-drawdown field test results from a shallow aquifer system

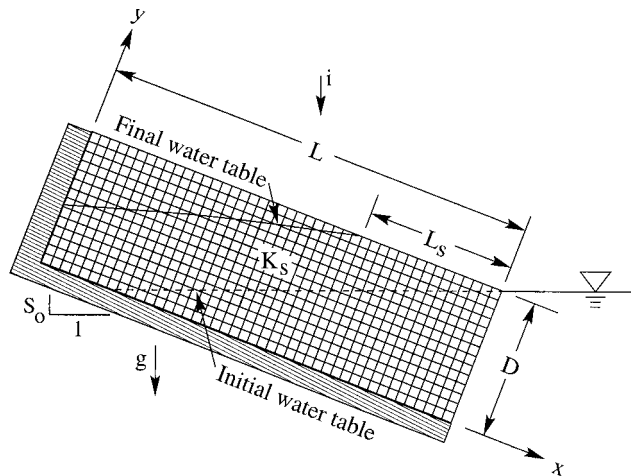


**Figure 1.** Conceptual drawing of the numerical simulation domain

quite accurately. The code was also used in simulation studies of the effect of geologic heterogeneity on groundwater recharge rates derived from environmental tracers by *McCord et al.* [1997].

## 5. Study Methodology

The sloping, vertically oriented two-dimensional domain selected to accomplish the study objectives is shown in Figure 1. A no-flow boundary condition was employed at the upslope end of the domain, representing a watershed divide. A constant head boundary condition was used at the downslope end, representing a stream. The upper surface of the model domain allowed infiltration and exfiltration, and the lower surface was a no-flow boundary, simulating an impermeable layer. The model domain was discretized into square finite difference grids, 10 cm on a side for soil depths greater than 1.0 m and 5 cm on a side for soil depths equal to or less than 1.0 m. These cell sizes were selected based on a sensitivity analysis that was performed to achieve stable, convergent, and accurate results as well as minimize simulation run time.

All VS2D simulations were started with an equilibrium soil water content profile above a horizontal water table that is established by a free water surface at the toe of the slope (see Figure 1). Initial soil water contents were calculated based on the head difference between the water table and the center of each computational volume element.

Non-Hortonian runoff production occurs on hillslopes with high infiltration capacities. Sand, therefore, was assumed to be the dominant soil. Representative van Genuchten parameters  $\alpha = 0.326$  m and  $m = 3.9$  were chosen for the media based on recommended values by *Lappala* [1981] and *van Genuchten* [1980]. The specific storage of the media is a required input parameter for VS2D. A value of  $1.0 \times 10^{-4}$  was chosen as a representative value for dense sandy gravel based on a literature review [*Domenico and Schwartz*, 1986; *de Marsily*, 1986; *Anderson and Woessner*, 1992]. The soil was assumed to be isotropic so that the influence of depth to impermeable layer  $D$  would not be “short-circuited” by less permeable soil layers. The residual water content and porosity of the soil were assumed to be 0.069 and 0.435, respectively.

VS2D allows exfiltration once the water table rises to the

surface of the domain. Monitoring the number of saturated surface cells at atmospheric pressure allows observation of the growth of saturated source areas in the model. The portion of the hillslope that is saturated is shown on Figure 1 as  $L_s$ . VS2D has no overland flow-routing capability. Water exfiltrated or precipitation falling directly on a saturated cell is removed from the surface and accounted for in mass balance computations. Overland flow routing is not needed to study this idealized hillslope because saturation must always proceed upward from the toe. This condition is insured by the fact that the hillslope properties are homogeneous and that the rainfall rates applied are much lower than the saturated hydraulic conductivity of the soil.

Four hillslope properties were varied: slope angle  $S_o$  (percent), depth to impermeable layer  $D$  (meters), uniform saturated hydraulic conductivity  $K_s$  ( $\text{cm h}^{-1}$ ), and slope length  $L$  (meters), together with the rainfall intensity  $i$  ( $\text{mm h}^{-1}$ ). We selected an initial value of  $S_o = 36\%$  to compare with the study by *Nieber and Warner* [1991]. Preliminary simulations showed that this slope angle is far too steep to produce any significant gain in saturated area for physically realistic rainfall rates. Therefore we selected smaller values of  $S_o$  from 2% to 20%. Values of soil thickness  $D$  were selected based on previous work by *Beasley* [1976], *Stagnitti et al.* [1986], and *Nieber and Warner* [1991]. *Nieber and Warner* [1991] used  $D = 1.0$  m for base conditions in numerical hillslope studies. *Beasley* [1976] observed clay layers at 1.8 m and 2.0 m in a field study. *Stagnitti et al.* [1986] observed soil thickness of 0.5 m in one small Connecticut watershed. We tested values of  $D$  from 0.5 m to 3.0 m. *Nieber and Warner* [1991] selected a slope length of 51 m for their base conditions. We tested three different slope lengths in this study: 15, 30, and 50 m.

This study was designed to simulate a hypothetical homogeneous hillslope with high infiltration capacities. Values of  $K_s$  tested were derived from *Morris and Johnson* [1967] and ranged from  $100 \text{ cm h}^{-1}$ , which represents fine sand, to  $1500 \text{ cm h}^{-1}$ , which represents coarse sand. These  $K_s$  values are higher than those typically seen in field studies with heterogeneous soils [*Hewlett and Hibbert*, 1967; *Stagnitti et al.*, 1992] but are, nonetheless, physically realistic and appropriate for use in this numerical study of a hypothetical homogeneous hillslope. Rainfall rates  $i$  tested were 10, 20, 30, 40, and  $50 \text{ mm h}^{-1}$ . In terms of runoff production mechanism the relative rainfall rate ( $i K_s^{-1}$ ) is an important variable. Relative rainfall rates less than 1.0 cannot produce Hortonian runoff on a heterogeneous hillslope. Values of relative rainfall rates tested in this study range from  $6 \times 10^{-4}$  to  $5 \times 10^{-2}$ . For this reason the study hillslope will only experience saturation from below.

## 6. Analytical Considerations

The degree of surface saturation at equilibrium for a homogeneous hillslope can be predicted by considering the distance from the top of the slope  $x$  where the water table will intersect the land surface under the action of steady state rainfall. The location of the intersection must coincide with the point along the slope that the downslope flux through the saturated zone is equal to the influx of rainfall above that point, and the saturated thickness is equal to the soil thickness. Assuming that the hydraulic gradient is equal to the land surface slope  $S_o$  at the point where the water table intersects the ground surface, this can be expressed mathematically as

$$ix = DK_s S_o. \quad (9)$$

With reference to Figure 1, considering that the fraction of the slope saturated  $\Lambda$  is related to  $x$  (assuming that  $x \leq L$ ) by

$$\Lambda = \frac{L_s}{L} = \left(1 - \frac{x}{L}\right) = 1 - \frac{DK_s S_o}{iL}, \quad (10)$$

it is clear that a slope of length  $L$  will not experience surface saturation unless the following is true (defining the parameter  $\Phi$ ):

$$\Phi = \frac{iL}{DK_s S_o} \geq 1.0. \quad (11)$$

Substituting the definition in (11) into (10), the fraction of the hillslope saturated at equilibrium is given by the following relation:

$$\Lambda = 1 - (1/\Phi). \quad (12)$$

The parameter  $\Phi$  may be interpreted as the ratio of the flux that tends to cause SSA formation ( $iL$ ) to the flux that tends to dissipate SSA formation ( $DK_s S_o$ ).  $\Phi$  also can be interpreted with slight modification as the ratio of the travel time in the saturated zone ( $L K_s^{-1} S_o^{-1}$ ) to the time required for rainfall to fill the available pore space neglecting groundwater flux ( $(\phi - \bar{\theta})Di^{-1}$ ), where  $\phi$  is the porosity of the medium and  $\bar{\theta}$  is the average volumetric water content. Equation (12) addresses only steady state saturation and does not reveal the nature of the temporal evolution of saturated source areas. Numerical model results are relied upon for this purpose.

## 7. Time to Steady State

Analysis of simulation results requires an objective reference time to evaluate the temporal evolution of saturated areas. The kinematic time to equilibrium for a nonconvergent, constant-slope hillslope with highly pervious soils can be analytically derived provided a number of assumptions are made. These assumptions include the following: Travel time from the land surface to the water table in the unsaturated zone is negligible; the average water table slope is equal to the land surface slope  $S_o$  [Beven, 1981]; the initial water content within the soil is spatially uniform; and the water table at no time intersects the land surface. Note that these assumptions are very limiting within the context of this study and therefore do not yield a general solution in the case of saturation excess runoff. The resulting equation for the kinematic time to equilibrium under the above limiting assumptions is

$$t_e \propto L/K_s S_o. \quad (13)$$

Equation (13) is not immediately applicable for the analysis presented in this paper because we are primarily interested in situations where the water table intersects the land surface. However, it is interesting to note that the rainfall rate does not appear in (13) because the flow velocity is independent of the saturated thickness under the assumed conditions.

The time to equilibrium for the idealized hillslope was determined numerically using VS2D simulations for a wide range of hillslope properties and rainfall rates. The time to equilibrium for a given hillslope configuration and rainfall rate was determined by applying rainfall at a constant rate and noting the elapsed time when the outflow from all control surfaces equaled 99.8% of the influx of rain. The fraction 99.8% is necessary because the storage within the hillslope asymptotically approaches the steady state value. The extent of surface

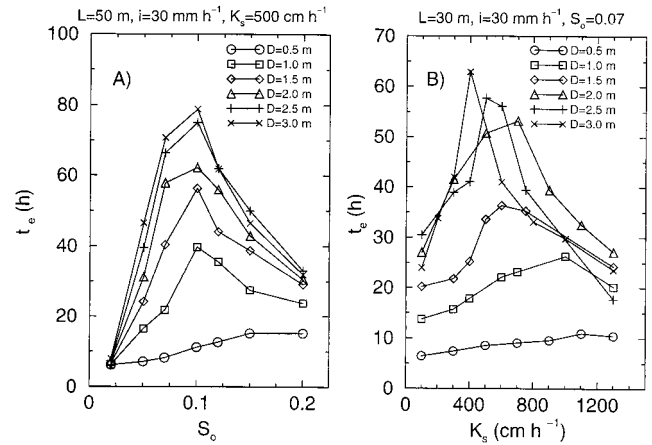


**Figure 2.** Effect of hillslope characteristics (a)  $S_o$  and (b)  $K_s$  on the time to equilibrium for various soil thicknesses  $D$  and fixed  $i$  and  $L$ .

saturation is not as reliable an indicator of steady state because an accurate determination of the fraction of the slope saturated at equilibrium would require finite difference cells considerably smaller than 5 to 10 cm, particularly for smaller slope angles.

## 8. Results

The influence of four hillslope parameters and the rainfall rate on the formation of saturated area was examined by holding four of the parameters constant while varying each parameter of interest. Simulations were run with constant rainfall intensity for a duration longer than the hillslope time to equilibrium for that rain rate.

### 8.1. Time to Equilibrium

In reality, equilibrium rarely occurs; the change in water table location within the hillslope is a slow process, compared with Hortonian runoff. During extreme events and times of constant influx of water (e.g., snowmelt) an equilibrium state can be approached. It is useful to consider the time to equilibrium within this context.

Figure 2 contains two plots that show the effect of changes in slope angle and saturated hydraulic conductivity on the time to equilibrium as determined by numerical simulation. Figure 2a shows that for the given hypothetical hillslope conditions,  $t_e$  increases with increasing slope up to a slope of approximately 10%. For slopes steeper than approximately 10%,  $t_e$  decreases with increasing slope angle for soils thicker than 0.5 m. With the shallowest soil tested, 0.5 m, there is a general but gradual increase in  $t_e$  with increasing slope over the range of slopes examined. Figure 2a also shows that  $t_e$  increases with soil thickness for all slope angles. For the shallowest slope angle tested,  $S_o = 0.02$ ,  $t_e$  is identical for all soil thicknesses for the given values of  $L$ ,  $i$ , and  $K_s$ .

Figure 2b shows that for fixed  $L$ ,  $i$ , and  $S_o$ , there is a saturated hydraulic conductivity that results in a maximum  $t_e$  for all values of soil thickness tested. As  $K_s$  changes from this value, there is a reduction in  $t_e$ . Investigation of the effects of slope length shows that  $t_e$  generally increases with increasing slope length as one would expect.

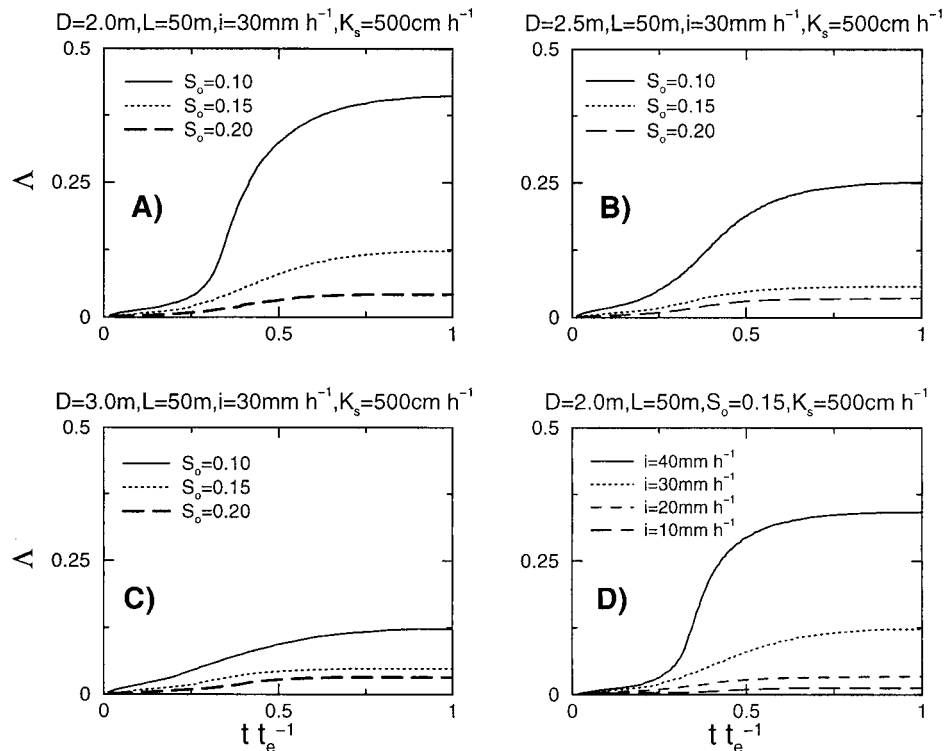


**Figure 3.** Temporal evolution of relative hillslope saturated area for three different soil thicknesses  $D$  equal to (a) 2.0, (b) 2.5, and (c) 3.0 m and (d) one slope subject to four different rainfall rates.

## 8.2. Slope Characteristics and Saturated Length

Plots of the fraction of hillslope saturated,  $\Lambda$ , versus  $t t_e^{-1}$  reveal the relative temporal response of hillslopes with different characteristics to constant rainfall. Examples of the effect of slope angle, soil thickness, and rainfall rate on the development of saturated area are shown in Figure 3. Figures 3a–3c show simulation results with three different soil thicknesses:  $D = 2.0, 2.5,$  and  $3.0$  m, respectively. Each of these plots contains results for three different slope angles,  $S_o = 0.1, 0.15,$  and  $0.20$ . The simulation results shown on these three plots are all derived from simulations with an isotropic saturated hydraulic conductivity  $K_s = 500 \text{ cm h}^{-1}$ , constant rainfall intensity  $i = 30 \text{ mm h}^{-1}$ , and slope length  $L = 50$  m. Figures 3a–3c show that steeper slopes have the smallest  $\Lambda$  at equilibrium. These three plots also indicate that as both  $D$  and  $S_o$  decrease, surface saturation increases nonlinearly.

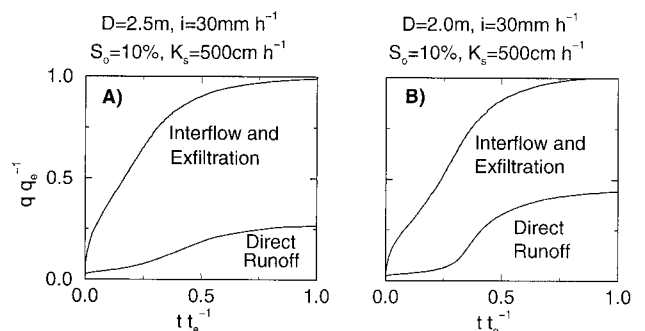
Comparing Figures 3a–3c, it is apparent that hillslopes with shallower soils are considerably more sensitive to  $S_o$  than those with deeper soils. It is also noteworthy that steep hillslopes (e.g., 20% slope) have very little saturated area at equilibrium for all soil thicknesses tested. The 20% angle hillslope with 2 m soil thickness has  $\Lambda = 0.05$  at equilibrium, while on the same hillslope with 10% slope angle  $\Lambda = 0.40$ . Comparing Figures 3a–3c also reveals that saturated areas on hillslopes with shallower soils and lower slope angles form more nonlinearly over time than those with deeper soils and steeper slope angles. Notice that in Figure 3a, with soil depth of 2.0 m,  $\Lambda$  increases from 0.10 to 0.30 between  $t t_e^{-1} = 0.33$  and  $t t_e^{-1} = 0.55$ . In Figure 3c, with  $D = 3$  m,  $\Lambda$  increases only from 0.05 to 0.08 over the same relative time period at the same slope angle.

Figure 3d illustrates nonlinear temporal response of the same hillslope subjected to four different rainfall rates. The

rate of growth of saturated area depends strongly on the rainfall rate. Notice that for  $i = 10 \text{ mm h}^{-1}$ ,  $\Lambda = 0.03$  at equilibrium, whereas for  $i = 40 \text{ mm h}^{-1}$ ,  $\Lambda = 0.3$ . This represents a tenfold increase in surface saturation due to a fourfold increase in rainfall. This ratio is not constant over the period  $0 \leq t \leq t_e$ , indicating significant nonlinearities in surface saturation with respect to rainfall rate.

Figure 4 shows outflow hydrographs separated into direct runoff and interflow components for the 10% slope-angle simulations shown in Figures 3a and 3b. Direct runoff is approximately 45% of the equilibrium discharge for a soil thickness of 2 m. The proportion of runoff occurring as direct runoff decreases to 26% as the soil thickness is increased to 2.5 m.

Model simulations were performed for cases where the isotropic, homogeneous hydraulic conductivity was assigned values ranging from 100 to 1500  $\text{cm h}^{-1}$ . At equilibrium, with  $L =$



**Figure 4.** Influence of soil depth on the fraction of runoff occurring as direct runoff.

50 m,  $D = 1.5$  m,  $S_o = 0.15$ , and  $i = 30$  mm h<sup>-1</sup>, for  $K_s = 400, 500,$  and  $750$  cm h<sup>-1</sup>,  $\Lambda = 0.49, 0.36,$  and  $0.06$ , respectively. For  $D = 2.0$  m, with all other variables remaining the same and  $K_s = 400, 500,$  and  $750$  cm h<sup>-1</sup>, the equilibrium  $\Lambda$  is  $0.29, 0.11,$  and  $0.03$ , respectively. In general, a decrease in hydraulic conductivity increases the amount of saturated area at equilibrium.

### 8.3. Storage Effects

VS2D simulation results for the entire parameter space were analyzed to investigate the relationship between equilibrium storage and  $\Lambda$  at equilibrium. This analysis requires two definitions. The final volume of water in the model domain at equilibrium  $V_f$  is calculated using

$$V_f = \int_0^L \int_0^D \theta \, dy \, dx, \quad (14)$$

and the maximum possible storage in the hillslope  $V_{\max}$  is calculated using

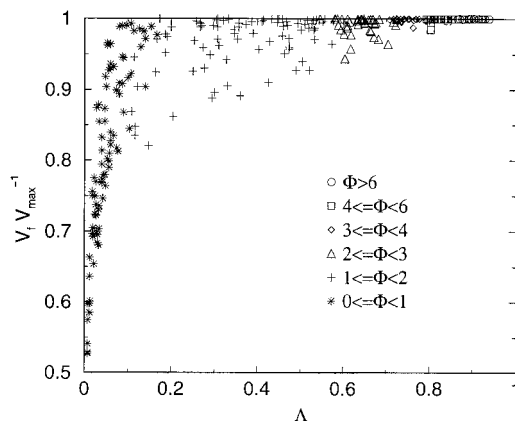
$$V_{\max} = \int_0^L \int_0^D \phi \, dy \, dx. \quad (15)$$

Figure 5 shows a plot of the relative storage  $V_f V_{\max}^{-1}$  in the hillslope versus  $\Lambda$  at equilibrium. Different symbols are used to denote ranges of values of the parameter  $\Phi$ . Figure 5 shows that there is no unique relation between  $V_f V_{\max}^{-1}$  and  $\Lambda$ . In fact, Figure 5 reveals that different hillslopes can have very different relative storage values and identical surface saturation. It is interesting to note that for  $\Phi$  less than 1.0, the relative storage within the hillslope can vary between 0.53 and 0.90 with  $\Lambda$  less than 0.10. Once  $\Phi$  exceeds 3.0, the relative storage is very close to 1.0, and  $\Lambda$  is greater than 0.7. Figure 6 shows a plot of relative storage versus  $\Phi$  and reveals that for any  $\Phi$  greater than 1.0, there is a significant likelihood that the relative storage will exceed 0.99.

## 9. Analysis and Discussion

### 9.1. Time to Equilibrium

The results shown in Figure 2 provide some insight into the influence of the relevant variables on the temporal response of nonconvergent, homogeneous constant-slope hillslopes. For a



**Figure 5.** Relative storage versus relative surface saturation at equilibrium.

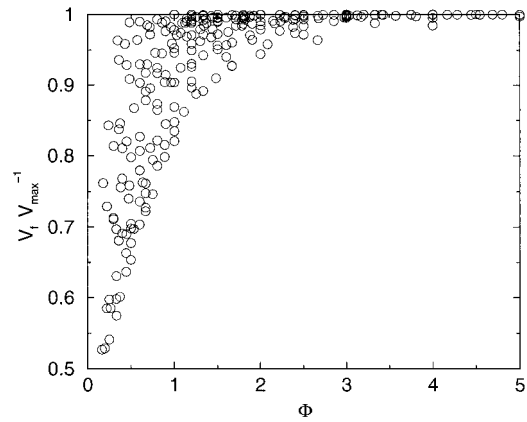


**Figure 6.** Relative storage versus the parameter  $\Phi$  at equilibrium.

given  $L, D, i,$  and  $K_s$ , there is a slope angle that results in a maximum  $t_e$  as shown in Figure 2a. The physical explanation for the existence of this maxima depends on the storage that must be filled to achieve equilibrium versus the ability of the hillslope to move water. As the slope angle approaches zero, the change in storage required to reach equilibrium also approaches zero. For this reason, the time to equilibrium is small for small slope angles. For higher slope angles ( $S_o > 10\%$ ) the change in storage required to reach equilibrium is small. Furthermore, steeper slopes produce larger flow velocities, resulting in a reduction of  $t_e$  compared with the maximum value. The parameter  $\Phi$  represents the ratio of the flux tending to cause saturated area formation to the flux tending to dissipate saturation. This physical argument suggests that the maximum  $t_e$  occurs when these two factors are in approximate balance near  $\Phi = 1.0$ . In fact, the maxima in Figure 2a, for soil thickness  $D = 1.0, 1.5, 2.0, 2.5,$  and  $3.0$  m, occur at  $\Phi = 3.0, 2.0, 1.5, 1.2,$  and  $1.0$ , respectively. Given the imposed initial condition (see Figure 1), thinner soils have smaller initial available storage ( $(\phi - \bar{\theta})Di^{-1}$ ), resulting in a smaller storage accumulation time ( $(\phi - \bar{\theta})Di^{-1}$ ) and hence larger  $\Phi$  for maximum  $t_e$  using the alternate interpretation of the parameter  $\Phi$  as discussed in section 6.

A similar case can be made for the existence of a  $t_e$  maxima in Figure 2b, which shows  $t_e$  plotted against  $K_s$  for a number of different soil thicknesses. As  $K_s$  goes to zero,  $t_e$  should approach zero (e.g., impervious surface). For very large  $K_s$  values the ability of the hillslope to convey water and reach equilibrium is large, resulting in smaller  $t_e$  values. However, at intermediate  $K_s$  values, the ability of the hillslope to transport water is only moderate yet high enough to allow significant changes in storage. The values of  $\Phi$  that correspond to the maxima shown in Figure 2b for soil depths of 1.0, 1.5, 2.5, and 3.0 m are 0.9, 1.0, 0.72, and 0.75, respectively, within the resolution of the results.

Figure 7 shows a plot of simulated  $t_e$  normalized by (13),  $L(K_s S_o)^{-1}$ , versus  $\Phi$ , with symbols denoting different values of  $S_o$ . Equation (13) overpredicts  $t_e$  in all cases. This is to be expected because (13) assumes a uniform initial soil moisture, while the VS2D simulations have a very nonuniform initial soil moisture state, with portions of the soil profile below the water table being saturated. There is a definite negative correlation between  $t_e K_s S_o L^{-1}$  and  $\Phi$  for  $\Phi$  greater than 1.0. As  $\Phi \rightarrow 0$ , the simulated  $t_e$  values approach the result predicted by (12).

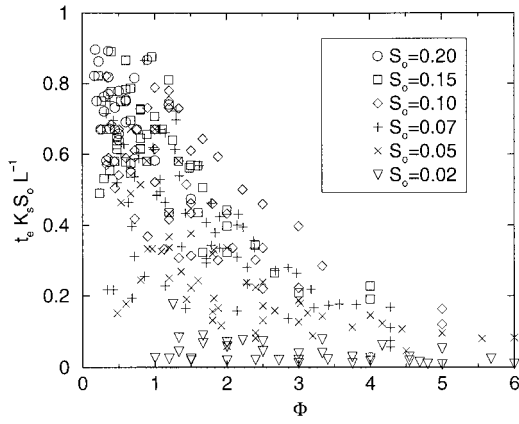


**Figure 7.** Results of numerically determined  $t_e$  normalized by theoretical  $t_e$  (equation (13)) versus parameter  $\Phi$ .

The points with the highest  $\Phi$  values in Figure 7 arise from simulations with  $S_o$  equal to 2%. This low slope angle has a very high initial moisture state and therefore requires less rainfall volume to reach steady state. Hillslopes with the smallest slope angles reach equilibrium most rapidly, as supported by Figure 2a.

## 9.2. Hillslope Properties

Figure 8 contains four plots of  $\Lambda$  versus  $\Phi$  for  $t/t_e^{-1} = 0.25, 0.50, 0.75,$  and  $1.0$  for all simulations performed. Each point on Figure 8 represents a different combination of  $i, D, K,$  and  $S_o$ . Different symbols are used to denote the different values of  $L$  tested to illustrate this difference. The temporal evolution of saturated source areas depends on specific hillslope geometry, the rainfall rate, and duration. For short duration rainfall  $t/t_e^{-1} = 0.25$ , there is moderate scatter in  $\Lambda$  for all values of  $\Phi$  as shown in Figure 8a. The maximum  $\Lambda$  observed in this case is approximately 0.2. As the rainfall duration increases, simulations with  $\Phi < 1$  approach equilibrium conditions, while simulations with larger  $\Phi$  values continue to exhibit considerable scatter as shown when  $t/t_e^{-1}$  equals 0.5 and 0.75 in Figure 8b and 8c. At  $t/t_e^{-1} = 1.0$  all slopes reach equilibrium, and the simulated  $\Lambda$  values become aligned with the analytically derived equilibrium  $\Lambda(\Phi)$  function (equation (12)) as shown in Figure 8d.

The derivation of (12) assumes that the slope of the water table is equal to the land surface slope at the point where the water table reaches the land surface. In reality, this is not the case. The water table slope is less than  $S_o$  and concave downward upstream from the intersection of the water table and land surface [Sloan and Moore, 1984]. Since the flow velocity in the saturated zone is proportional to the water table slope, the downslope velocity is less than that assumed in (12). For this reason the analytical relation shown in Figure 8d underpredicts  $\Lambda$  for a given  $\Phi$  by approximately 5% for  $\Phi > 2$ . When  $1 < \Phi < 2$ , the underestimation increases to approximately 10%.

The scatter in Figure 8 for  $t/t_e^{-1}$  less than 1.0 is explained by considering the physics of the rising water table. For small slope angles the available storage profile in the hillslope is a thin, triangular wedge over most of  $L$ . In steeper slopes the available storage profile is more rectangular in shape with a triangular portion near the toe of the slope. Water table rise has two potential sources which can be explained from conservation principles. The first is due to an increase in discharge in

the flow direction due to rainfall, which creates a corresponding convective increase in the saturated thickness  $y$  in the flow direction:

$$\frac{\partial y}{\partial x} = \frac{i}{\phi K_s S_o}. \quad (16)$$

Equation (16) indicates that this source of water table rise occurs for all rainfall rates and decreases with increasing  $K_s$  and  $S_o$ . The second source of water table rise is dominant when the rainfall rate becomes large in the following equation:

$$\phi \frac{\partial y}{\partial t} = i - \phi K_s S_o \frac{\partial y}{\partial x}. \quad (17)$$

When the rainfall rate is large compared to the second term on the right-hand side of (17), a significant local water table rise occurs. On steep slopes, where the initial available storage profile is more rectangular in shape, this significant water table rise can cause the point where the water table intersects the land surface to propagate upslope very rapidly. This point is illustrated in Figure 9, which shows the trajectory of saturated area  $\Lambda$  versus  $t/t_e^{-1}$  for different slope angles over ranges of  $\Phi$ . Each curve on the plots in Figure 9 represents a different simulation with different hillslope characteristics and rainfall rate, while the line style denotes the slope angle. Very steep trajectories indicate rapid temporal changes in  $\Lambda$  on steeper slopes when  $\Phi > 1.0$ . These rapid increases result when the rising water table is nearly parallel to the ground surface on steeper slopes. For values of  $\Phi$  greater than 6, the influence of the initial storage profile is reduced, and the temporal change of  $\Lambda$  is more linear.

## 10. Conclusions

This study represents a mechanistic analysis of the formation of saturated source areas on a topographically nonconvergent,

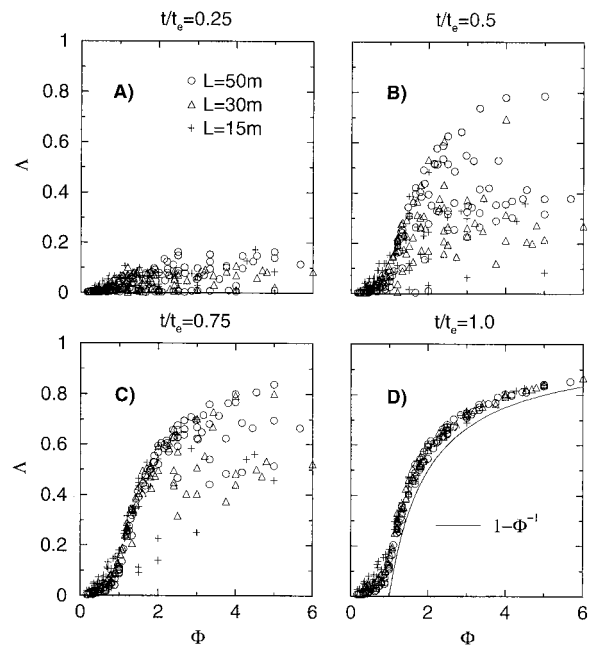


**Figure 8.** Percentage of hillslope saturated versus dimensionless parameter  $\Phi$  for different degrees of hillslope equilibrium:  $t/t_e^{-1}$  equal to (a) 0.25, (b) 0.50, (c) 0.75, and (d) 1.0.

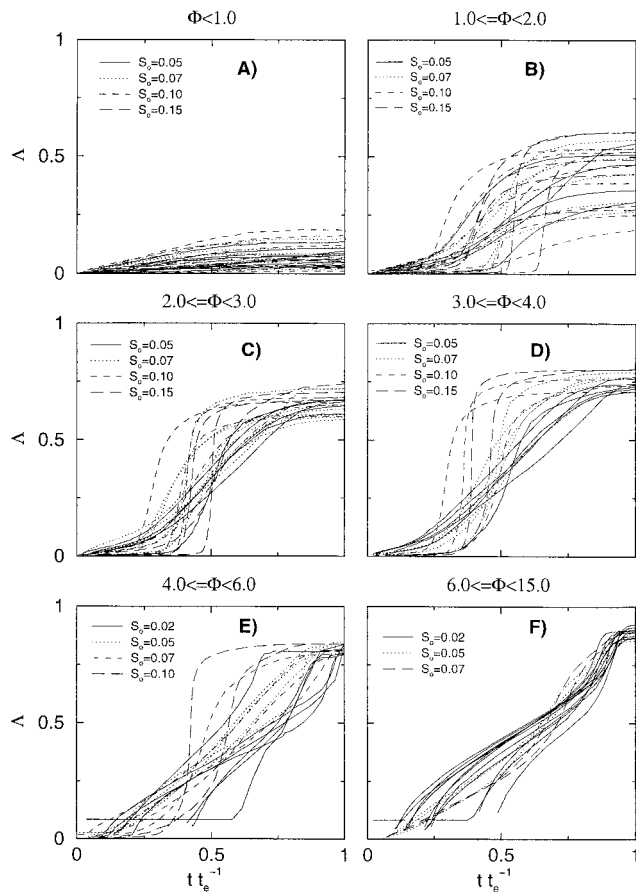


**Figure 9.** Trajectory of saturated area versus time for different values of slope angle over ranges of the parameter  $\Phi$ : (a)  $\Phi < 1.0$ , (b)  $1.0 \leq \Phi < 2.0$ , (c)  $2.0 \leq \Phi < 3.0$ , (d)  $3.0 \leq \Phi < 4.0$ , (e)  $4.0 \leq \Phi < 6.0$ , and (f)  $6.0 \leq \Phi < 15.0$ .

constant sloped, homogeneous hillslope. The rainfall rates used in this study ( $10 \leq i \leq 50 \text{ mm h}^{-1}$ ) are significantly less than the tested saturated hydraulic conductivity values ( $100 \leq K_s \leq 1500 \text{ cm h}^{-1}$ ), insuring that saturation excess runoff was produced. The parameter space explored in this study is quite large, over a significant range of physically realistic hillslope parameter values. Slopes with lengths of 15, 30, and 50 m were tested. Soil depths from 0.5 to 3.0 m were tested, with slope angles that varied from 2 to 20%. In all, over 400 two-dimensional unsteady, unsaturated flow simulations were performed over the parameter space, with the parameter  $\Phi$  ranging from 0.1 to 15 with most simulations performed with  $0.5 \leq \Phi \leq 2.0$ .

The dimensionless parameter  $\Phi = iLD^{-1}K_s^{-1}S_o^{-1}$  has important implications for the formation of saturated source areas. This parameter can be interpreted in two ways. The first is that the parameter represents the ratio of the flux tending to cause saturation ( $iL$ ) to the flux tending to dissipate saturated source areas ( $DK_sS_o$ ). The second interpretation is that the parameter represents the ratio of the hillslope response time ( $LK_s^{-1}S_o^{-1}$ ) to the storage accumulation time ( $(\phi - \theta)Di^{-1}$ ). Both of these interpretations are useful for analyzing the temporal nature of SSA formation.

The temporal aspects of saturated area formation are analyzed with respect to the time to equilibrium  $t_e$ . The time to equilibrium generally increases with increasing soil depth and

slope length. For a given rainfall rate, soil thickness, and slope length, there are  $K_s$  and  $S_o$  values that result in a maximum  $t_e$ . This maximum occurs near  $\Phi = 1.0$  on soils deeper than 1 m. This indicates that the time to equilibrium is longest when the factors that tend to generate surface saturation are in approximate balance with the factors that tend to dissipate surface saturation. In the case of shallower soils ( $D < 1.0 \text{ m}$ ) the available soil water storage is small, and the ratio of the hillslope response time ( $LK_s^{-1}S_o^{-1}$ ) to storage accumulation time ( $(\phi - \theta)Di^{-1}$ ) determines the formation equilibrium conditions. The temporal evolution of saturated area is highly nonlinear with time, particularly for hillslopes with shallower soils and higher rainfall intensities.

Under constant intensity rainfall, saturated area formation is greatest for slopes with shallower soils, smaller slope angles, longer slope lengths, and smaller average hydraulic conductivities. Direct runoff is a larger portion of the total runoff on hillslopes with shallower soils, particularly for higher degrees of equilibrium ( $t_e^{-1}$  greater than 0.4). The dimensionless parameter  $\Phi$  is a similarity parameter for SSA extent on non-convergent constant-slope hillslopes at equilibrium, as shown in Figure 8d. Hillslope saturation increases nonlinearly with increasing  $\Phi$ .

Differences in hillslope properties and rain rate have a large effect on the temporal evolution of SSAs when  $t < t_e$ . Figure 9 shows six plots of the temporal evolution of  $\Lambda$  for  $0 \leq t \leq t_e$  for different slope angles over ranges of  $\Phi$  values. When  $\Phi$  is less than 1.0,  $\Lambda$  is generally less than 0.2, and the increase in  $\Lambda$  over time is very gradual for all slope angles investigated. However, when  $\Phi$  is greater than or equal to 1.0, the temporal evolution of  $\Lambda$  becomes much more variable. Steeper slopes tend to have smaller  $\Phi$  values and therefore have a smaller fraction of saturated area than a shallower slope when all other properties are the same. However, when  $\Phi$  becomes large because of high relative rainfall rates  $iK_s^{-1}$ , the time rate of change of saturated area is much larger on steeper slopes than on the milder slopes as shown in Figures 9b–9e. When  $\Phi$  is greater than 6.0, the rainfall rate completely overwhelms the transport of water in the saturated zone, and the time rate of change of surface saturation becomes much more linear as shown in Figure 9f.

The results presented in this paper offer a fresh look at a subject that has been examined by a number of researchers. The influence of physically based, quantifiable, hillslope properties on the formation of saturated source areas is explored. The hillslope simulated in this study is simple; it is homogeneous, constant-sloped, and nonconvergent, with uniform rainfall. However, the results of this study illustrate that even under greatly simplified conditions, there is tremendous natural variability in the formation of saturated source areas.

**Acknowledgments.** The authors gratefully acknowledge support for this research by the U.S. Army Research Office under grant DAAH04-96-1-0026 and the Connecticut Department of Environmental Protection under contract AGR 7-1-97. The authors thank R. W. Healy of the U.S. Geological Survey for his assistance with the application of VS2D. Glenn S. Warner of the University of Connecticut and David P. Ahlfeld of the University of Massachusetts (formerly University of Connecticut) provided useful guidance. Constructive review comments by Stephen E. Silliman and M. Todd Walter improved this paper.

## References

Anderson, M. G., and T. P. Burt (Eds.), *Process Studies in Hillslope Hydrology*, 450 pp., John Wiley, New York, 1990.

- Anderson, M. P., and W. W. Woessner, *Applied Groundwater Modeling*, 381 pp., Academic, San Diego, Calif., 1992.
- Barros, A. P., D. Knapton, M. C. Wang, and C. Y. Kuo, Runoff in shallow soils under laboratory conditions, *J. Hydraul. Eng.*, 4(1), 28–37, 1999.
- Beasley, R. S., Contribution of subsurface flow from the upper slopes of forested watersheds to channel flow, *Soil Sci. Soc. Am. J.*, 40, 955–959, 1976.
- Betson, R. P., What is watershed runoff?, *J. Geophys. Res.*, 69(8), 1541–1552, 1964.
- Beven, K. J., Kinematic subsurface stormflow, *Water Resour. Res.*, 17(5), 1419–1424, 1981.
- Beven, K. J., and M. J. Kirkby, A physically based, variable contributing area model of basin hydrology, *Hydrol. Sci. Bull.*, 24(1), 43–69, 1979.
- Boughton, W. C., Systematic procedure for evaluating partial areas of watershed runoff, *J. Irrig. Drain. Eng.*, 116(1), 83–98, 1990.
- Bras, R. L., *Hydrology An Introduction to Hydrologic Science*, 643 pp., Addison-Wesley-Longman, Reading, Mass., 1990.
- Brooks, R. H., and A. T. Corey, Hydraulic properties of porous media, *Hydrol. Pap. 3*, Colo. State Univ., Fort Collins, 27 pp., 1964.
- Chorley, R. J., The hillslope hydrologic cycle, in *Hillslope Hydrology*, edited by M. J. Kirkby, pp. 1–42, John Wiley, New York, 1978.
- de Marsily, G., *Quantitative Hydrogeology*, 440 pp., Academic, San Diego, Calif., 1986.
- Domenico, P. A., and F. W. Schwartz, *Physical and Chemical Hydrogeology*, 440 pp., Academic, San Diego, Calif., 1986.
- Dunne, T., and R. D. Black, An experimental investigation of runoff production in permeable soils, *Water Resour. Res.*, 6(2), 478–490, 1970.
- Frankenburger, J. R., E. S. Brooks, M. T. Walter, M. F. Walter, and T. S. Steenhuis, A GIS based variable source area hydrology model, *Hydrol. Processes*, 13(6), 805–822, 1999.
- Freeze, R. A., Role of subsurface flow in generating surface runoff, 2, Upstream source areas, *Water Resour. Res.*, 8(5), 1272–1283, 1972.
- Halford, K. J., Effects of unsaturated zone on aquifer test analysis in a shallow-aquifer system, *Ground Water*, 35(3), 512–522, 1997.
- Haverkamp, R., M. Vauclin, J. Tovina, P. J. Wierenga, and G. Vachaud, A comparison of numerical simulation models for one-dimensional infiltration, *Soil Sci. Soc. Am.*, 41, 285–294, 1977.
- Healy, R. W., Simulation of solute transport in variably saturated porous media with supplemental information on modifications to U.S. Geological Survey's computer program VS2D, *U.S. Geol. Surv. Water Resour. Invest. Rep.*, 90-4025, 1990.
- Hewlett, J. D., and A. R. Hibbert, Factors affecting the response of small watersheds to precipitation in humid areas, in *International Symposium on Forest Hydrology (1965)*, Pennsylvania State University edited by W. E. Sopper and H. W. Lull, pp. 275–290, Pergamon, Tarrytown, N.Y., 1967.
- Hornberger, G. M., K. J. Beven, B. J. Cosby, and D. E. Sappington, Shenandoah watershed study: Calibration of a topography-based, variable contributing area hydrological model to a small forested catchment, *Water Resour. Res.*, 21(12), 1841–1850, 1985.
- Horton, R. E., The role of infiltration in the hydrologic cycle, *Eos Trans. AGU*, 14, 446–460, 1933.
- Iorgulescu, I., and J. P. Jordan, Validation of TOPMODEL on a small Swiss catchment, *J. Hydrol.*, 159, 255–273, 1994.
- Kirkby, M. J. (Ed.), *Hillslope Hydrology*, John Wiley, New York, 1978.
- Lappala, E. G., Modeling of water and solute transport under variably saturated conditions, in *State of the Art: Modeling and Low-Level Waste Management, An Interagency Workshop, Denver, Colorado, 1980 Proceedings*, pp. 81–137, U. S. Govt. Print. Off., Washington, D.C., 1981.
- Lappala, E. G., R. W. Healy, and E. P. Weeks, Documentation of computer program VS2D to solve the equations of fluid flow in variably saturated porous media, *U.S. Geol. Surv. Water Resources Invest. Rep.*, 83-4099, 1993.
- McCord, J. T., C. A. Gotway, and S. H. Conrad, Impact of geologic heterogeneity on recharge estimation using environmental tracers: Numerical modeling investigation, *Water Resour. Res.*, 33(6), 1229–1240, 1997.
- McDonnell, J. J., J. Freer, R. Hooper, C. Kendall, D. Burns, K. Beven, and J. Peters, New method developed for studying flow on hillslopes, *Eos Trans. AGU*, 77(47), 465 and 472, 1996.
- Morris, D. A., and A. I. Johnson, Summary of Hydrologic and Physical Properties of Rock and Soil Materials, as Analysed by the Hydrologic Laboratory of the U.S. Geologic Survey, 1948–1960, *U.S. Geol. Surv. Water Supply Pap.*, 1839-D, 1967.
- Nieber, J. L., and M. F. Walter, Two-dimensional soil moisture flow in a sloping rectangular region: Experimental and numerical studies, *Water Resour. Res.*, 17(6), 1722–1730, 1981.
- Nieber, J. L., and G. S. Warner, Soil pipe contribution to steady subsurface stormflow, *Hydrol. Processes*, 5, 329–344, 1991.
- Obled, C., J. Wendling, and K. Beven, The sensitivity of hydrological models to spatial rainfall patterns: An evaluation using observed data, *J. Hydrol.*, 159, 305–333, 1994.
- O'Brien, A. L., Alternative approaches to understanding runoff in small watersheds, *J. Boston Soc. Civ. Eng.*, 69(2), 303–319, 1983.
- O'Loughlin, E. M., Saturation regions in catchments and their relations to soil and topographic properties, *J. Hydrol.*, 53, 229–246, 1981.
- O'Loughlin, E. M., Prediction of surface saturation zones in natural catchments by topographic analysis, *Water Resour. Res.*, 22(5), 794–804, 1986.
- Sloan, P. G., and I. D. Moore, Modeling surface and subsurface stormflow on steeply-sloping forested watersheds, *Water Resour. Res.*, 20(12), 1815–1822, 1984.
- Southeastern Forest Experiment Station, Report for 1961, annual report, pp. 62–63, Asheville, N. C., 1961.
- Stagnitti, F., M. B. Parlange, T. S. Steenhuis, and J.-Y. Parlange, Drainage from a uniform soil layer on a hillslope, *Water Resour. Res.*, 22(5), 631–634, 1986.
- Stagnitti, F., J.-Y. Parlange, T. S. Steenhuis, M. B. Parlange, and C. W. Rose, A mathematical model of hillslope and watershed discharge, *Water Resour. Res.*, 28(8), 2111–2122, 1992.
- Steenhuis, T. S., M. Winchell, J. Rossing, J. A. Zollweg, and M. F. Walter, SCS runoff equation revisited for variable-source runoff areas, *J. Irrig. Drain. Eng.*, 121(3), 234–238, 1995.
- Stone, H. L., Iterative solution of implicit approximations of multidimensional partial differential equations, *SIAM J. Numer. Anal.*, 5, 530–558, 1968.
- Tennessee Valley Authority, Area-stream factor correlation, *Bull. Int. Assoc. Sci. Hydrol.*, 10(2), 22–37, 1965.
- van Genuchten, M. T., A closed-form for predicting the hydraulic conductivity of unsaturated soils, *Soil. Sci. Soc. Am. J.*, 44, 892–898, 1980.
- Watts, B. A., *Formation of Saturated Areas on Hillslopes With Shallow Soils*, M.S. thesis, 90 pp., Univ. of Conn., Storrs, 1998.
- Wigmosta, M. S., L. W. Vail, and D. P. Lettenmaier, A distributed hydrology-vegetation model of complex terrain, *Water Resour. Res.*, 30(6), 1665–1680, 1994.
- Wolock, D. M., G. M. Hornberger, K. J. Beven, and W. G. Campbell, The relationship of catchment topography and soil hydraulic characteristics to lake alkalinity in the United States, *Water Resour. Res.*, 25(5), 829–837, 1989.
- Zollweg, J. A., W. J. Gburek, and T. S. Steenhuis, SmoRMod—A GIS-integrated rainfall-runoff model, *Trans. ASAE*, 39(4), 1299–1307, 1996.

F. L. Ogden, Department of Civil and Environmental Engineering, University of Connecticut, Storrs, CT 06269. (ogden@enr.uconn.edu)  
B. A. Watts, 68R Lovers Lane, Nantucket, MA 02554.

(Received August 4, 1999; revised March 29, 2000; accepted March 30, 2000.)